Inorg. Chem. **2008**, *47*, 3893−3902

Insights into DNA Binding of Ruthenium Arene Complexes: Role of Hydrogen Bonding and π Stacking

Konstantinos Gkionis, James A. Platts,* and J. Grant Hill

School of Chemistry, Cardiff University, Park Place, Cardiff CF10 3AT, U.K.

Received December 20, 2007

Density functional theory (DFT) methods are used to investigate the binding of ruthenium arene complexes, proposed as promising anticancer drugs, to isolated nucleobases. This shows a clear preference for binding at guanine over any other base and an approximately 100 kJ mol^{-1} difference in binding between guanine and adenine in the gas phase, while binding to cytosine and inosine are intermediate in energy between these extremes. Solvation reduces binding energies and the discrimination between bases but maintains the overall pattern of binding. DFT and ab initio data on arene−base interactions in the absence of ruthenium show that stacking and hydrogen-bonding interactions play a significant role but cannot account for all of the energy difference between bases observed. Atoms-in-molecules analysis allows further decomposition of binding energies into contributions from covalent-binding, hydrogen-bonding, and π-stacking interactions. Larger arenes undergo stabilizing stacking interactions, whereas N−H···X hydrogen bonding is independent of arene. Pairing of guanine to cytosine is affected by ruthenium complexation, with individual hydrogen-bonding energies being altered but the overall pairing energy remaining almost constant.

Introduction

Noncovalent interactions are important throughout chemistry and the life sciences. The nucleic acids DNA and RNA are classic examples of this,[1–5] with hydrogen bonding and π stacking between determination of the structure and stability of nucleic acids.[6,7] Selective recognition of molecules by nucleic acids often depends on such interactions, for example, in intercalation of planar aromatic molecules between bases of DNA,[8–18] a promising strategy for anticancer drug design.[10–13] DNA is also an attractive target for metal-based anticancer drugs[19–27] and is the main biological target of the successful drug cisplatin. Covalent binding to

* To whom correspondence should be addressed. E-mail: platts@cf.ac.uk. Phone: +44-2920-874950. Fax: +44-2920-874030.

(1) Fohrer, J.; Hennig, M.; Carlomagno, T. *J. Mol. Biol.* **2006**, *356*, 280–287.
(2) Watson, J. D.; Crick, F. H. C. *Nature* **1953**, *171*, 737–738.
(3) Ghosh, A.; Bansal, M. *J. Mol. Biol.* **1999**, *294*, 1149–1158.
(4) Pan, B.; Shi, K.; Sundaralingam, M. *J. Mol. Biol.* **2006**, *363*, 451–459.
(5) Yakovchuk, P.; Protozanova, E.; Frank-Kamenetskii, M. D. *Nucl. Acids Res.* **2006**, *34*, 564–574.
(6) Hernandez, B.; Baumruck, V.; Leulliota, N.; Gouyetted, C.; Huynh-Dinhd, T.; Ghomia, M. *THEOCHEM* **2003**, *651*, 67–74.
(7) Aldrich-Wright, J. R.; Vagg, S. R.; Williams, P. A. *Coord. Chem. Rev.* **1997**, *166*, 361–389.
(8) Řeha, D.; Kabeláč, M.; Ryjáček, F.; Šponer, J.; Šponer, J. E.; Elstner, M.; Suhai, S.; Hobza, P. *J. Am. Chem. Soc.* **2002**, *124*, 3366–3766.
(9) Choudhury, J. R.; Bierbach, U. *Nucl. Acids Res.* **2005**, *33*, 5622–5632.
(10) Cusumano, M.; Di Pietro, M. L.; Giannetto, A. *Inorg. Chem.* **1999**, *38*, 1754–1758.
(11) Wall, R. K.; Shelton, A. H.; Bonaccorsi, L. C.; Bejune, S. A.; Dubé, D.; McMillin, D. R. *J. Am. Chem. Soc.* **2001**, *123*, 11480–11481.
(12) Hecht, C.; Friedrich, J.; Chang, T.-C. *J. Phys. Chem. B* **2004**, *108*, 10241–10244.
(13) Armitage, B.; Koch, T.; Frydenlund, H.; Ørum, H.; Schuster, G. B. *Nucl. Acids Res.* **1998**, *26*, 715–720.
(14) Dempcy, R. O.; Kutyavin, I. V.; Mills, A. G.; Lukhtanov, E. A.; Meye, R. B. *Nucl. Acids Res.* **1999**, *27*, 2931–2937.
(15) Baruah, H.; Bierbach, U. *Nucl. Acids Res.* **2003**, *31*, 4138–4146.
(16) Shieh, H.-S.; Berman, H. M.; Dabrow, M.; Neidle, S. *Nucl Acids Res.* **1980**, *8*, 85–97.
(17) Nakatani, K.; Matsuno, T.; Adachi, K.; Hagihara, S.; Saito, I. *J. Am. Chem. Soc.* **2001**, *123*, 5695–5702.
(18) Ferguson, L. R.; Denny, W. A. *Mutat. Res./Fundam. Mol. Mech. Mutagenesis* **2007**, *623*, 14–23.
(19) Baker, E. S.; Manard, M. J.; Gidden, J.; Bowers, M. T. *J. Phys. Chem. B* **2005**, *109*, 4808–4810.
(20) Clarke, M. J.; Zhu, F.; Frasca, D. R. *Chem. Rev.* **1999**, *99*, 2511–2533.
(21) Collery, P.; Keppler, B.; Madoulet, C.; Desoize, B. *Crit. Rev. Oncology/Hematol.* **2002**, *42*, 283–296.
(22) Calamai, P.; Guerri, A.; Messori, L.; Orioli, P.; Speroni, G. P. *Inorg. Chim. Acta* **1999**, *285*, 309–312.
(23) Berners-Price, S. J.; Mirabelli, C. K.; Johnson, R. K.; Mattern, M. R.; McCabe, F. L.; Faucette, L. F.; Sung, C.-M.; Mong, S.-M.; Sadler, P. J.; Crooke, S. T. *Cancer Res.* **1986**, *46*, 5486–5493.
(24) Tiekink, E. R. T. *Crit. Rev. Oncol./Hematol.* **2002**, *42*, 225–248.
(25) Katsaros, N.; Anagnostopoulou, A. *Crit. Rev. Oncol./Hematol.* **2002**, *42*, 297–308.
(26) Meléndez, E. *Crit. Rev. Oncol./Hematol.* **2002**, *42*, 309–315.
(27) Evangelou, A. M. *Crit. Rev. Oncol./Hematol.* **2002**, *42*, 249–265.

10.1021/ic702459h CCC: $40.75
Published on Web 04/08/2008

DNA, chiefly guanine and adenine, leads to structural distortion and ultimately cell death.[28–32] Recently developed ruthenium(II) complexes of the type $[(\eta^6\text{-arene})Ru^{II}(en)Cl][PF_6]$ (en = ethylenediamine) show promising anticancer activity,[33] comparable to or better than platinum anticancer complexes. Chemical and spectroscopic studies[34,35] reveal a stronger preference for guanine than was observed with platinum-based drugs, with experimental NMR data suggesting that hydrogen bonding to guanine could explain the observed preferential binding.

The size of the arene ligand strongly affects the activity;[33] arenes containing two or more rings, such as, for example, biphenyl (bip) or tetra- or dihydroanthracene (tha and dha), have crystal structures[34] that reveal π-stacking interactions between the arene and base, in addition to hydrogen bonds. Hence, the ruthenium(II) arene complexes can be considered as potential intercalators.[34,36] Experiments on DNA duplexes with ruthenium(II) arene complexes showed that the tha complex has a cancer cell cytotoxicity of approximately 20 times higher than that of a ruthenium cymene complex.[37] It is important to note, however, that while DNA binding is believed to be the mechanism of action, other factors such as cell uptake will affect the cytotoxicity and could be strongly dependent on the nature of the arene. Studies on DNA duplexes reveal the importance of the arene ligand, which distorts the DNA duplex through intercalation in the biphenyl complex (although partially saturated arenes such as tha and dha may not be "true" intercalators) and through steric interactions in the cymene complex.[38] The same study showed that the distortion caused by the cymene complex was extended to more nucleic acid pairs than the distortion caused by the tha complex.

Benchmark ab initio calculations on nucleobase and amino acid pairs[39–41] indicate that description of π stacking in particular is a challenging theoretical problem, requiring large basis sets and accurate treatment of electron correlation. Such methods are capable of impressive accuracy,[42–44] but unfortunately computational requirements prevent application to larger systems such as the ruthenium(II) complexes considered here. Density functional theory (DFT) is a computationally attractive alternative to ab initio methods, with lower computational cost and more favorable scaling with molecular size. A variety of approaches have been taken for the description of noncovalent interactions using DFT.[8,40,44–50] Waller et al. recently tested Becke's half-and-half functional (BHandH), which yields satisfactory results for π-stacked systems, although it overestimates the hydrogen-bond strength.[51] In previous work by our group, BHandH was applied successfully in combination with atoms-in-molecules (AIM) analysis for the study of DNA oligonucleotides in the gas phase[52] and the binding of cisplatin to DNA oligonucleotides.[53] This combined approach is computationally efficient and provides both qualitative and quantitative information of the interactions present. In this work, we use the same approach to quantify the noncovalent interactions when ruthenium(II) complexes of the type $[(\eta^6\text{-arene})Ru^{II}(en)]^{n+}$ bind to nucleobases, and where necessary, benchmark these against other methods.

Computational Methods

Initial DFT geometry optimization and calculation of the binding energy were carried out using the *Gaussian03*[54] software, employing the BHandH[55] functional. BHandH consists of half of the exact (Ex^{HF}) and half of the local spin density approximation (Ex^{LSDA}) for the exchange energy, along with the Lee–Yang–Parr (LYP)[56] expression for the correlation energy (Ec^{LYP}). As mentioned above, BHandH has been shown to yield geometries and energies comparable to those of more accurate methods and to experiment, where available, for π-stacked systems and for cisplatin−nucleobase adducts.[51–53] The $O(N^3)$ scaling of the DFT methods allows application to relatively large systems, for which more traditional ab initio methods such as Møller–Plesset or coupled cluster theories are not feasible. This also allows use of a basis set adequate for the description of nonbonded interactions. The geometries of all complexes were optimized at the BHandH/6-31+G** level. The basis set superposition error (BSSE) in binding energies was accounted for using the counterpoise correction of Boys and Bernardi.[57] In all calculations, the Ru atom was described with the

(28) Desoize, B.; Madoulet, C. *Crit. Rev. Oncol./Hematol.* **2002**, *42*, 317–325.
(29) Sherman, S. E.; Lippard, S. J. *Chem. Rev.* **1987**, *87*, 1153–1181.
(30) Mansy, S.; Chu, G. Y. H.; Duncan, R. E.; Tobias, R. S. *J. Am Chem. Soc.* **1978**, *100*, 607–616.
(31) Gonzalez, V. M.; Fuertes, M. A.; Alonso, C.; Perez, J. M. *Mol. Pharmacol.* **2001**, *59*, 657–663.
(32) Natile, G.; Marzilli, L. G. *Coord. Chem. Rev.* **2006**, *250*, 1315–1331.
(33) Morris, R. E.; Aird, R. E.; Murdoch, P.; del, S.; Chen, H.; Cummings, J.; Hughes, N. D.; Parsons, S.; Parkin, A.; Boyd, G.; Jodrell, D. I.; Sadler, P. J. *J. Med. Chem.* **2001**, *44*, 3616–3621.
(34) Chen, H.; Parkinson, J. A.; Parsons, S.; Coxall, R. A.; Gould, R. O.; Sadler, P. J. *J. Am. Chem. Soc.* **2002**, *124*, 3064–3082.
(35) Chen, H.; Parkinson, J. A.; Morris, R. E.; Sadler, P. J. *J. Am. Chem. Soc.* **2003**, *125*, 173–186.
(36) Novakova, O.; Chen, H.; Vrana, O.; Rodger, A.; Sadler, P. J.; Brabec, V. *Biochemistry* **2003**, *42*, 11544–11554.
(37) Novakova, O.; Kasparkova, J.; Bursova, V.; Hofr, C.; Vojtiskova, M.; Chen, H.; Sadler, P. J.; Brabec, V. *Chem. Biol.* **2005**, *12*, 121–129.
(38) Liu, H.-K.; Wang, F.; Parkinson, J. A.; Bella, J.; Sadler, P. J. *Chem.—Eur. J.* **2006**, *12*, 6151–6165.
(39) Jurečka, P.; Šponer, J.; Černy, J.; Hobza, P. *Phys. Chem. Chem. Phys.* **2006**, *8*, 1985–1993.
(40) Dąbkowska, I.; Gonzalez, H. V.; Jurečka, P.; Hobza, P. *J. Phys. Chem. A* **2005**, *109*, 1131–1136.
(41) Hobza, P.; Šponer, J. *J. Am. Chem. Soc.* **2002**, *124*, 11802–11808.
(42) Rejnek, J.; Hobza, P. *J. Phys. Chem. B* **2007**, *111*, 641–645.
(43) Jurečka, P.; Šponer, J.; Šerný, J.; Hobza, P. *Phys. Chem. Chem. Phys.* **2006**, *8*, 1985–1993.
(44) Dąbkowska, I.; Jurečka, P.; Hobza, P. *J. Chem. Phys.* **2005**, *122*, 204322.
(45) Elstner, M.; Hobza, P.; Frauenheim, T.; Suhai, S.; Kaxiras, E. *J. Chem. Phys.* **2001**, *114*, 5149–5155.
(46) van der Wijst, T.; Guerra, C. F.; Stewart, M.; Bickelhaupt, F. M. *Chem. Phys. Lett.* **2006**, *426*, 415–421.
(47) Zhao, Y.; Truhlar, D. G. *J. Chem. Theory Comput.* **2007**, *3*, 289–300.
(48) Zhao, Y.; Schultz, N. E.; Truhlar, D. G. *J. Chem. Theory Comput.* **2006**, *2*, 364–382.
(49) von Lilienfeld, O. A.; Tavernelli, I.; Sebastiani, D.; Rothlisberger, U. *Phys. Rev. Lett.* **2004**, *93*(15), 153004.
(50) Lin, I.-C.; von Lilienfeld, O. A.; Coutinho-Neto, M. D.; Tavernelli, I.; Rothlisberger, U. *J. Phys. Chem. B* **2007**, *111*, 14346–14354.
(51) Waller, M. P.; Robertazzi, A.; Platts, J. A.; Hibbs, D. E.; Williams, P. A. *J. Comput. Chem.* **2006**, *27*, 491–504.
(52) Robertazzi, A.; Platts, J. A. *J. Phys. Chem. A* **2006**, *110*, 3992–4000.
(53) Robertazzi, A.; Platts, J. A. *Chem.—Eur. J.* **2006**, *12*, 5747–5756.
(54) Frisch, M. J.; et al. *Gaussian03*, revision C.02; Gaussian, Inc.: Wallingford, CT, 2004.
(55) Becke, A. D. *J. Chem. Phys.* **1993**, *98*, 1372–1377.
(56) Lee, C.; Yang, W.; Parr, R. G. *Phys. Rev. B* **1988**, *37*, 785–789.
(57) Boys, S. F.; Bernardi, F. *Mol. Phys.* **1970**, *19*, 553–566.

SDD basis set and ECP.[58] Following these BHandH geometry optimizations, additional calculations were performed using the M05 functional via the *NWChem*[59] software package.

Because of the size of the complexes studied, computational requirements for harmonic frequency calculation exceeded the resources available to us for the largest complexes. Tests on smaller compounds show that inclusion of zero-point and/or thermal energy correction does not noticeably affect trends in the binding energy (see the Supporting Information, Table S1). We therefore present binding energies uncorrected for these quantities and concentrate more on a comparison between combinations of arene and base rather than on absolute values. For the same reason, explicit solvent molecules were not included. The aqueous solution of complexes and their separated moieties was estimated using the polarizable continuum model (PCM) approach,[60–62] employing a dielectric constant of 78.39 and atomic radii from the UFF force field.[63] In this way, the binding energy corrected for hydration effects was estimated.

Further calculations were carried out on certain fragments of the studied complexes, as explained in the Results and Discussion section, with the DF-LMP2[64] and DF-SCSN-LMP2[65] (herein referred to simply as SCSN) methodologies using Dunning's aug-cc-pVTZ basis set.[66] DF-LMP2 is a modification of the local MP2[67,68] approach (LMP2), including density fitting approximations of the electron repulsion integrals. Excitation domains for the local approximation were generated in the same fashion as those in previous SCSN investigations.[65] The use of a local electron correlation treatment minimizes the BSSE, and hence counterpoise corrections are unnecessary. The SCSN approach is based on Grimme's spin component scaling method (SCS-MP2),[69] in which the parallel and antiparallel spin components are scaled by different parameters (see ref 69 for further discussion). The scaling parameters for SCSN have been optimized for stacked nucleic acid–base pairs and have been shown to produce high-quality interaction energies for a range of noncovalent interactions.[65,70] The DF-LMP2 and SCSN calculations were carried out using the MOLPRO package.[71]

AIM analysis was performed on wave functions generated at the same level as geometry optimizations. Topological analysis of the electron density (ρ) was carried out using the *AIM2000* package[72–74] in order to determine the critical points (CPs) at which the gradient of the density ($\nabla\rho$) is zero. Among these extrema, our interest is focused on the (3, −1) or bond CPs (BCPs), which are characterized by a minimum along the internuclear direction and maxima in the perpendicular directions. Properties calculated at BCPs are informative about the interactions present,[75] and such analysis has been widely employed in investigations of intra- and intermolecular interactions.[52,53,76–81] For instance, positive $\nabla^2\rho(r)$ with low $\rho(r)$ typically indicates "closed-shell" interaction, such as ionic or hydrogen bonds, while positive $\nabla^2\rho(r)$ with relatively large $\rho(r)$ corresponds to covalent or "shared" interactions. Apart from this qualitative picture of the interactions in a system, AIM analysis can provide quantitative information. Linear correlations have been observed between the total electron density at BCPs and the energy of hydrogen-bonding[82] and π-stacking[51] interactions. Calibration of densities calculated at the BHandH level against binding energies gives linear correlations with standard deviations of 2.0 kJ mol^{-1} for stacked complexes and 4.4 kJ mol^{-1} for hydrogen bonds.

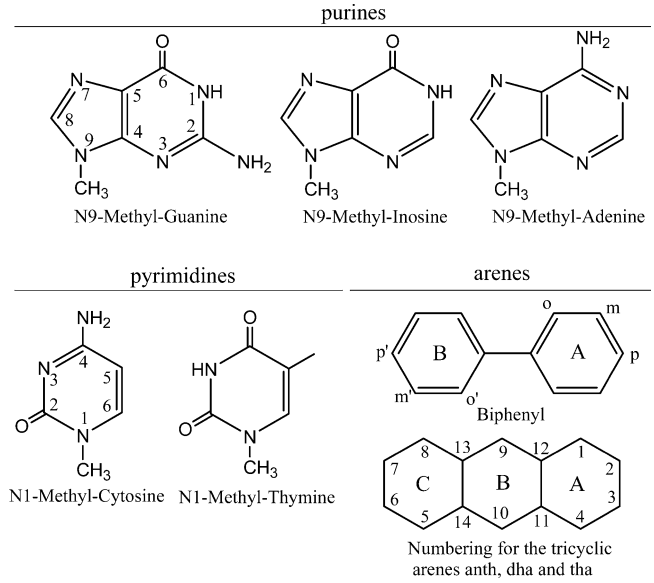

Figure 1. Arenes and bases studied, including numbering scheme.

Results and Discussion

Figure 1 shows the nucleobases and arenes considered, along with atom numbering. The N9 methyl purines and N1 methyl pyrimidines are referred to simply as G, I, A and C, T, respectively. The A rings of bip, dha, and tha are those η^6- coordinated to the Ru atom. In addition to these arenes,

(58) Andrae, A.; Hausserman, U.; Dolg, M.; Stoll, H.; Preuss, H. *Theor. Chim. Acta* **1990**, *77*, 123–141.
(59) (a) Bylaska, E. J.; et al. *NWChem, A Computational Chemistry Package for Parallel Computers*, version 5.0; Pacific Northwest National Laboratory: Richland, WA, 2006. (b) Kendall, R. A.; Apra, E.; Bernholdt, D. E.; Bylaska, E. J.; Dupuis, M.; Fann, G. I.; Harrison, R. J.; Ju, J.; Nichols, J. A.; Nieplocha, J.; Straatsma, T. P.; Windus, T. L.; Wong, A. T. *Comput. Phys. Commun.* **2000**, *128*, 260–262.
(60) Miertus, S.; Scrocc, E.; Tomasi, J. *Chem. Phys.* **1981**, *55*, 117.
(61) Miertus, S.; Tomasi, J. *Chem. Phys.* **1982**, *65*, 239–245.
(62) Cossi, M.; Barone, V.; Cammi, R.; Tomasi, J. *Chem. Phys. Lett.* **1996**, *255*, 327–335.
(63) Rappé, A. K.; Casewit, C. J.; Colwell, K. S.; Goddard, W. A., III; Skiff, W. M. *J. Am. Chem. Soc.* **1992**, *114*, 10024.
(64) Werner, H.-J.; Manby, F. R.; Knowles, P. J. *J. Chem. Phys.* **2003**, *118*, 8149–8160.
(65) Hill, J. G.; Platts, J. A. *J. Chem. Theory Comput.* **2007**, *3*, 80–85.
(66) Kendall, R. A.; Dunning, T. H.; Harrison, R. J. *J. Chem. Phys.* **1992**, *96*, 6796–6806.
(67) Schütz, M.; Hetzer, G.; Werner, H.-J. *Chem. Phys.* **1999**, *111*, 5691–5705.
(68) Hetzer, G.; Schütz, M.; Stoll, H.; Werner, H.-J. *J. Chem. Phys.* **2000**, *113*, 9443–9455.
(69) Grimme, S. *J. Chem. Phys.* **2003**, *118*, 9095–9102.
(70) Antony, J.; Grimme, S. *J. Phys. Chem. A* **2007**, *111*, 4862–4868.
(71) Werner, H.-J.; et al. *MOLPRO, a package of ab initio programs*, version 2006.1.
(72) Bader, R. W. F. *Atoms in Molecules: A Quantum Theory*; Clarendon Press: Oxford, U.K., 1990.
(73) Bader, R. W. F. *Pure Appl. Chem.* **1988**, *60*, 145–155.
(74) Biegler-König, J.; Schönbohm, J. *J. Comput. Chem.* **2002**, *23*, 1489–1494.
(75) Bader, R. F. W.; Essen, J. *J. Chem. Phys.* **1984**, *80*, 1943–1960.
(76) Oliveira, B. G.; Pereira, F. S.; de Araujo, R. C. M. U.; Ramos, M. N. *Chem. Phys. Lett.* **2006**, *427*, 181–184.
(77) Raissi, H.; Nowroozi, A.; Mohammdi, R.; Hakimi, M. *Spectrochim. Acta A* **2006**, *65*, 605–615.
(78) Palusiak, M.; Rudolf, B.; Zakrzewski, J.; Pfitzner, A.; Zabel, M.; Grabowski, S. J. *J. Organomet. Chem.* **2006**, *691*, 3232–3238.
(79) Wojtulewski, S.; Grabowski, S. *Chem. Phys.* **2005**, *309*, 183–188.
(80) Oliveira, B. G.; Araujo, R. C. M. U.; Carvalho, A. B.; Ramos, A. B. *Chem. Phys. Lett.* **2007**, *433*, 390–394.
(81) Mohajeri, M.; Karimi, E. *THEOCHEM* **2006**, *774*, 71–76.
(82) Oldfield, S. PPh.D. Thesis, Cardiff University, Cardif, U.K., 2007.

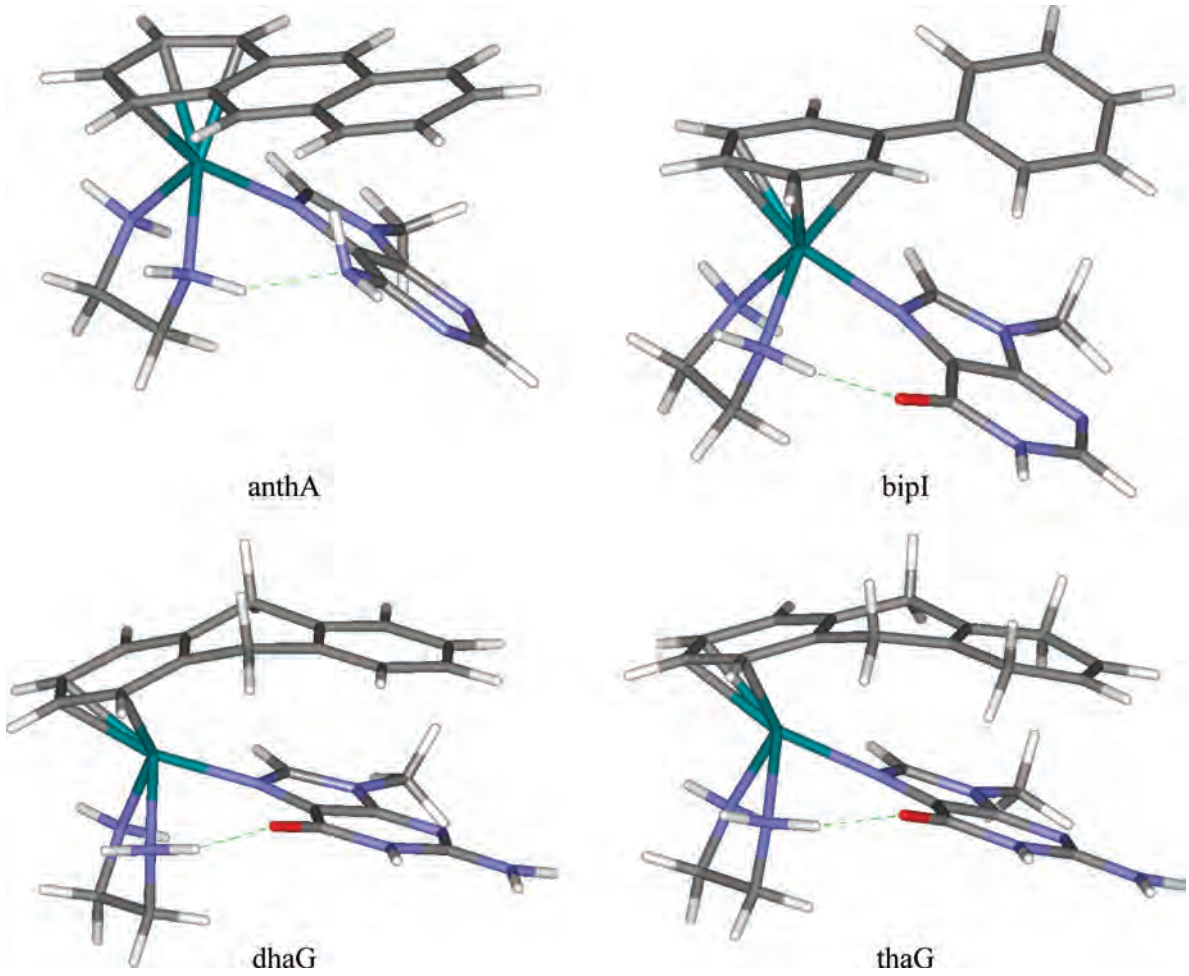

Figure 2. Optimized geometries of selected compounds.

Table 1. Selected Optimized Geometrical Parameters and Comparison with Experiment[a]

	Ru−N_{base} (Å)	Ru−N_{en} (Å)	Ru−arene (Å)	N···X (Å)	N−H···X (deg)	θ^b (deg)	ϕ^c (deg)	R^d (Å)
benG	2.094	2.097	1.707	2.68	162.8		29.6	
anthG	2.095	2.083	1.750	2.70	162.8	0.0	28.9	5.095
bipG	2.092 (2.120)	2.096 (2.116)	1.715 (1.677)	2.67 (2.799)	164.8(162.9)	29.6[e] (13.7)	24.8[f] (23.8)	4.011[f] (3.801)
dhaG	2.092 (2.117)	2.110 (2.118)	1.711 (1.680)	2.70 (2.840)	161.8(163.1)	29.5 (31.9)	4.7 (3.1)	3.39 (3.31)
thaG	2.096 (2.128)	2.098 (2.127)	1.710 (1.683)	2.71 (2.812)	162.2(163.3)	24.7 (27.8)	6.9 (3.3)	3.34 (3.45)

[a] Reported as the BHandH optimized value on first line and the experimental X-ray value (where available) in parenthesis. [b] Arene hinge angle on C9−C10 atoms. [c] Arene−base interplanar angle. [d] Arene (ring C)−base (6-membered ring) centroid−centroid distance. [e] Ring A−ring B propeller twist. [f] ϕ and R between ring B of bip and a 5-membered ring of G.

which have been studied experimentally,[34,35] we have also examined the parent anthracene molecule, which lacks the flexibility of dha and tha and is therefore not expected to bind as tightly or undergo π stacking to the same extent.

Optimized structures of selected complexes are displayed in Figure 2: all structures, as well as optimized Cartesian coordinates, can be found in the Supporting Information. These geometries show both covalent bonding to Ru and N−H···X hydrogen bonds between the en ligand (donor) and O or N atoms of the bases (acceptors). These hydrogen bonds are ubiquitous throughout all complexes studied, with the O6 of G and I, N6 of A, O2 of C, and O2 and O4 of T acting as acceptors to the en N−H donor. Given the previous success of BHandH in describing π stacking,[51–53] it is encouraging to note that the arene ligands bip, dha, and tha are positioned over the nucleobases, in a manner similar to that in reported crystal structures.[34] Table 1 summarizes some key geometrical features of the optimized structures and, where possible, compares these with the crystal structures reported in ref 34. In general, the agreement is good, with Ru−N_{base} and Ru−N_{en} distances within 0.02 Å of the experimental values and Ru−arene distances approximately slightly longer than experimental data. The tendency of BHandH to overestimate hydrogen bond strengths (and, hence, underestimate lengths by ca. 0.1 Å) is apparent from these comparisons, but this is a systematic error and so should have a smaller effect on the trend in binding energies. The mutual orientation of arene and guanine rings is well reproduced, in terms of both the separation between mean planes (R) and the angular orientation of the arenes over the nucleobases. The latter is described by the hinge angle (θ) on the C9–C10 atoms for the anth, dha, and tha ligands and the arene−base interplanar angle (φ).

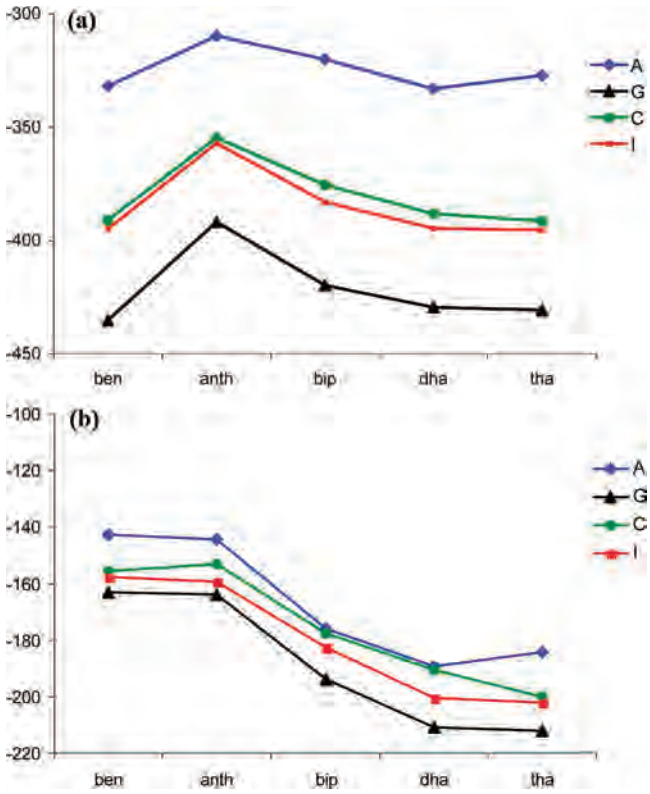

Figure 3. Counterpoise-corrected binding energies for A, G, C, and I in (a) the gas phase and (b) a PCM aqueous solution.

Table 2. Counterpoise-Corrected Binding Energies at the BHandH/6-31+G**(SDD) Level in the Gas Phase and an Aqueous Solution (kJ mol^{-1})[a]

base/arene	ben	anth	bip	dha	tha
A	−331.83	−309.71	−320.05	−333.02	−327.15
	−142.57	−144.59	−175.94	−189.21	−184.26
G	−435.15	−391.82	−419.75	−429.46	−430.70
	−163.08	−163.76	−193.87	−210.88	−212.11
C	−390.97	−354.66	−375.49	−388.13	−391.38
	−155.56	−153.30	−177.55	−190.36	−199.97
I	−394.75	−357.06	−383.03	−394.58	−395.34
	−157.68	−159.39	−182.60	−200.34	−202.18
T	−1115.25	−1056.10	−1078.17	−1094.36	−1098.60
GC	−486.03				−482.53

[a] First line = gas phase; second line = PCM aqueous solution.

Table 3. Binding Energies (kJ mol^{-1}) at the M05/6-31+G*/SDD Level

base/arene	ben	anth	bip	dha	tha
A	−245.50	−211.25	−216.77	−219.63	−211.60
G	−345.21	−296.61	−311.87	−313.02	−314.92
C	−293.12	−251.49	−264.25	−269.66	−264.73
I	−305.46	−260.62	−274.33	−277.34	−276.37

Counterpoise-corrected binding energies of bases to ruthenium complexes for all considered combinations of base and arene are reported in Table 2. The relative trends for A, C, G, and I bases are more clearly displayed in Figure 3. Complexes with guanine are bound much more tightly than are complexes of the remaining neutral nucleobases. This is in agreement with NMR studies[35] of complexes with [(η^6-bip)Ru(en)]$^{2+}$, which show that the reactivity decreases in the order G > I, T > C > A. Thymine is not included in Figure 3 because this can only bind as the N3-deprotonated anion, giving rise to much larger binding energies that are not comparable to those for the remaining neutral bases. The

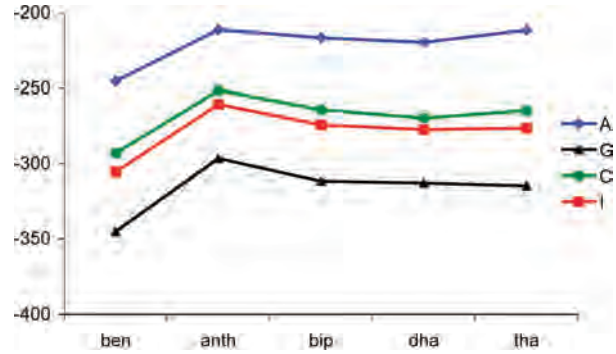

Figure 4. M05 binding energies for A, G, C, and I (kJ mol^{-1}).

gas-phase acidity of thymine has been reported as 1452 kJ mol^{-1},[83] such that in the absence of solvent binding of thymine to ruthenium arenes is predicted to be energetically unfavorable. The solvent will clearly have a larger effect on the relative energies of charged metal and ligand moieties than on the remaining complexes with neutral bases, rendering comparisons based on gas-phase data useless. We therefore have not considered thymine complexes in any subsequent analysis but will address the problem of including a solvent in subsequent work.

Comparison of binding energies for A and G complexes is particularly interesting because the nucleophilic sites of these bases are available for complexation in duplex DNA and are therefore the primary sites of metalation. The latter are found to be more stable by approximately 100 kJ mol^{-1}, no matter which arene ligand is considered. The equivalent comparison for platinum complexes has been calculated previously at ca. 63 kJ mol^{-1} using various theoretical methods and basis sets.[29,30,84–86] These data are again in complete agreement with the experiment, which indicates greater selectivity for G over A for ruthenium than for platinum complexes.[34] Solvation reduces binding energies by 200–300 kJ mol^{-1} across the board, perhaps unsurprisingly because complexes are separated into a free base and an uncoordinated ruthenium fragment. More interestingly, the large difference between binding to G and A is reduced in an aqueous solution, with an average differences of 21.5 kJ mol^{-1}. Baik et al. reported similar trends for cisplatin and assigned this to preferential solvation of G and the accessibility to a solvent of polar groups in A complexes, resulting in an energy difference of 19.2 kJ mol^{-1}.[85] Thus, the differential binding of G and A of these ruthenium arene complexes is suggested to be closer to that observed for cisplatin in an aqueous solution than that in the gas phase.

It has been suggested that the discrimination of G and A is due to the strong N−H···O hydrogen bond in complexes with G and to repulsion between amino groups of en and A. However, our optimized geometries indicate that hydrogen bonds are ubiquitous, with amino groups of A and C adopting

(83) Chen, E. C. M.; Herder, C.; Chen, E. S. *J. Mol. Struct.* **2006**, *798*, 126–133.
(84) Robertazzi, A.; Platts, J. A. *Inorg. Chem.* **2005**, *44*, 267–274.
(85) Baik, M.-H.; Friesner, R. A.; Lippard, S. J. *J. Am. Chem. Soc.* **2003**, *125*, 14082–14092.
(86) Zeizinger, M.; Burda, J. V.; Leszczynski, J. *Phys. Chem. Chem. Phys.* **2004**, *6*, 3585–3590.

a nonplanar geometry that allows N to act as a hydrogen-bond acceptor, in accordance with experimental and theoretical findings.[87–92] The sum of the angles around the amino $-NH_2$ atom for the A and C complexes was used in previous work to quantify this nonplanarity and is reported in the Supporting Information. In A complexes, these angles sum to around 335°, indicative of relatively strong hydrogen bonding, whereas in C complexes, these angles sum to ca. 355°, suggesting less reorientation due to hydrogen bonding.

The ubiquity of hydrogen bonds between amino groups of the en ligand and bases and the intermediate stability of the inosine complex suggest that the observed selectivity for guanine is not driven solely by N−H···O6 hydrogen bonding. It is evident from Figure 2, and from experimental X-ray and NMR studies,[34,35] that the complexes adopt conformations in which arenes are oriented over the bases, giving rise to additional stabilizing ring–ring stacking interactions. Table 2 and Figure 3 show that the binding energy follows the order anth > tha > dha > bip, i.e., increases with the size of the arene and with a more parallel, face-to-face orientation of the arene and base. This broadly agrees with the observation that cytotoxic activity of $[\eta^6$-arene)Ru(en)$]^{2+}$ complexes is increased with an increase in the size of the arene,[33] which also involves the ability to intercalate between DNA base pairs.[34,36] Thus, for these ligands at least, the importance of π stacking seems clear.

Anthracene has not been studied experimentally and was included in our theoretical study to examine the effect of arene rigidity. All anthracene complexes studied show weaker binding to a given base than any other arene considered. This seems most likely to be attributed to the lack of flexibility of the anth ligand, which prevents it from adopting a favorable positioning over the bases, that would allow for further stacking interactions. The reduced binding energy in the anth complexes (between 10 and 40 kJ mol^{-1}) is on the order expected for stacking interactions between DNA bases.[8,41,93–96] On the other hand, the relative twist of the two benzene rings in bip and the sp^3 character of the C9 and C10 atoms of dha and tha offer the required flexibility for developing stacking interactions between arenes and bases.

A clear exception to this trend is observed for complexes with benzene as the arene. Surprisingly, the binding energy of benzene complexes is comparable to that of dha and tha for all of the studied nucleobases. In the gas phase, benzene complexes have binding energies comparable to those of the tha complexes. Because stacking interactions should not be present in these complexes, the origin of this stability is not clear and will be explored in more detail below. However, in an aqueous solution, this apparently anomalous behavior is not present, and benzene shows behavior similar to that of anthracene. The lack of intercalative ability[34,36] of monocyclic arenes has been studied experimentally[37] with *p*-cymene (*p*-isopropyltoluene) as a ligand, in which distortion and thermal destabilization of DNA was found.

Table 4. Arene−Base BHandH Binding Energies (kJ mol^{-1})

	ben	anth	bip	dha	tha
A	+3.54	−15.01	−11.63	−17.03	−16.91
G	+2.10	−3.36	−15.87	−26.01	−27.43
I	+2.48	−5.20	−16.76	−26.76	−27.76
C	−6.51	−7.51	−20.57	−30.65	−36.19

To probe the origin of these binding energies in more detail, further calculations were carried out on fragments of the whole complexes. Two sets of fragments were identified: (i) with the Ru(en) moiety removed to leave just the arene and base and (ii) with the base removed to leave a $[\eta^6$-arene)Ru(en)$]^{2+}$ fragment. Both sets of fragments were fixed at the overall complex geometries. The former should shed light on stacking and other direct interactions between the arene and base, while the latter can be used to monitor the electronic effect of arene on the metal center and its potential interaction with ruthenium. Table 4 reports BHandH counterpoise-corrected arene−base binding energies, which confirm that interactions with benzene as the arene are small and, in most cases, slightly destabilizing. Interactions with anthracene are also generally small but stabilizing, although rather large stabilization is observed for adenine. Interestingly, this anthracene−adenine combination is also relatively stable from the data reported in Table 2. The more flexible arenes bip, dha, and tha show increased arene−base stabilization, increasing with the same trend as that seen for the overall binding energy for a given base. It seems clear, therefore, that the observed trend in binding energy against arene can be explained by these noncovalent interactions, with the obvious exception of benzene.

In order to test the performance of BHandH, additional calculations on the same arene−base fragments were performed at the DF-LMP2 and SCSN levels, using the aug-cc-pVTZ basis set. The binding energies obtained are shown in Table 5, and a comparison with BHandH for the tha complexes is illustrated in Figure 5. All three methods show the same trend in binding energy, but as is well-known, DF-LMP2 significantly overestimates the stacking energies. Excellent agreement between the BHandH and SCSN results is observed, with a root-mean-square error between these methods of just 3.2 kJ mol^{-1}. For the purines A, G, and I, BHandH values are slightly less negative (∼2.5 kJ mol^{-1}) than SCSN values, whereas with cytosine as the base, the BHandH energy drops below the SCSN value. The tendency of BHandH to overestimate hydrogen-bond energies may be the cause of this change; however, the same drop in energy is observed in the benzene series, for which no hydrogen bonds should be present.

(87) Vlieghe, D.; Sponer, J.; van Meervelt, L. *Biochemistry* **1999**, *38*, 16443–16451.
(88) Hovorun, D. M.; Gorb, L.; Leszczynski, J. *Int. J. Quant. Chem.* **1999**, *75*, 245–253.
(89) Sponer, J.; Hobza, P. *Int. J. Quant. Chem.* **1996**, *57*, 959–970.
(90) Sponer, J.; Hobza, P. *J. Phys. Chem.* **1994**, *98*, 3161–3164.
(91) Bludský, O.; Šponer, J.; Leszczynski, J.; Špirko, V.; Hobza, P. *J. Chem. Phys.* **1996**, *105*, 11042–11050.
(92) Luisi, B.; Orozco, M.; Sponer, J.; Luque, F. J.; Shakked, Z. *J. Mol. Biol.* **1998**, *279*, 1123–1136.
(93) Jurecka, P.; Hobza, P. *J. Am. Chem. Soc.* **2003**, *125*, 15608–15613.
(94) Sponer, J.; Gabb, H. A.; Leszczynski, J.; Hobza, P. *Biophys. J.* **1997**, *73*, 76–87.
(95) Leininger, M. L.; Nielsen, I. M. B.; Colvin, M. E.; Jannsen, C. L. *J. Phys. Chem. A* **2002**, *106*, 3850–3854.
(96) Yanson, I. K.; Teplitsky, A. B.; Sukhodub, L. F. *Biopolymers* **1979**, *18*, 1149–1170.

Table 5. Arene−Base SCSN and DF-LMP2 Binding Energies (kJ mol^{-1})

	ben		anth		bip		dha		tha	
	DF-LMP2	SCSN	DF-LMP2	SCSN	DF-LMP2	SCSN	DF-LMP2	SCSN	DF-LMP2	SCSN
A	+1.51	+5.24	−26.14	−18.82	−25.62	−16.41	−43.61	−26.89	−34.80	−19.10
G	−0.88	+3.00	−21.44	−13.05	−30.48	−20.99	−52.51	−36.81	−44.42	−30.10
I	−3.25	+1.68	−23.80	−14.98	−32.13	−22.67	−52.98	−37.62	−43.66	−30.27
C	−8.03	−3.11	−20.19	−12.57	−31.19	−22.72	−46.55	−33.63	−43.63	−31.36

Consideration of the second set of fragments goes some way to explaining the apparently anomalous behavior of benzene complexes. Orbital energies of each [η^6-arene)-Ru(en)]$^{2+}$ complex were calculated at both HF and DFT levels. An image of the lowest unoccupied molecular orbital (LUMO) of the benzene complex is shown in Figure 6: similar plots are observed for all other complexes. The LUMO of the benzene-containing fragment is markedly lower in energy (−0.424 au) than any of the remaining fragments (−0.376 to −0.396 au). On this basis, one would expect better overlap of benzene complexes with the highest occupied molecular orbital of the incoming base, and hence a stronger covalent bond, than with other arenes. This will be investigated in more depth, using AIM methods, below.

As well as complexes with single nucleobases, we have also studied two complexes of ruthenium with the guanine−cytosine Watson–Crick base pair. In both cases, the binding energies of ruthenium to the base pairs are approximately 50 kJ mol^{-1} greater than those for the analogous guanine complexes. This enhancement of the binding energies is reminiscent of the results for cisplatin complexes.[84] As well as the binding energy to ruthenium, the pairing energy of G with C, and the effect of ruthenium binding, can be calculated from these results. The pairing energy of free GC is 84.10 kJ mol^{-1}, a value that is little changed in the benGC complex (87.04) or the thaGC complex (83.62). A more detailed analysis of the observed effects on the GC pair, again using AIM analysis, will be discussed below.

From these results, it is apparent that the high selectivity of the studied ruthenium(II) complexes toward guanine cannot be fully understood by simple structural criteria. The fact that all nucleobases act as hydrogen-bond acceptors suggests that the interplay of all interactions gives rise to the observed selectivity. In order to decompose the interactions present and hence to explore this interplay of covalent bonding, hydrogen bonding, and π stacking, we turn to AIM analysis. Figure 7 displays molecular graphs for selected complexes. One point that is immediately apparent is that Ru−arene bonding is not present between all six arene atoms, but instead in most cases only three Ru−arene BCPs are found. This bonding pattern is not unusual for transition-metal sandwich complexes and has been observed by Palusiak et al.[78] in π complexes of tungsten, molybdenum, and iron. These authors suggest that this may be due to the use of ECPs rather than all-electron basis sets. Given the lack of such basis sets for ruthenium, we have little choice but to continue with this approach, and in any case, Ru−arene bonding is not the main focus of this investigation.

AIM analysis results in no arene−base interactions in any benzene complex and progressively more in anth, bip, dha, and tha complexes. This analysis reveals both stacking and hydrogen-bonding arene−base interactions, the strength of which can be estimated from properties of the relevant BCPs. In this way, the interactions can be decomposed into covalent bonding of the bases to ruthenium, hydrogen bonding between bases and en, and hydrogen bonding and π stacking between bases and arenes. Table 6 summarizes this AIM analysis for all complexes considered and lists the number of the arene−base hydrogen-bonding and stacking BCPs observed in each complex. More details of individual interactions, such as those between the en ligand and the purine and pyrimidine bases, can be found in the Supporting Information.

Table 7 also quantifies the strengths of the various noncovalent interactions, including both arene−base and en−base. This indicates that the hydrogen bonds from en $-NH_2$ ligands to O6 of guanine are the most stabilizing, closely followed by those to inosine. These are in the range 29–33 kJ mol^{-1} for G and 28–32 kJ mol^{-1} for I, with only a small effect coming from the nature of the arene. The strongest such hydrogen bond is found in bipG, approximately of equal strength to that in bipI. The strength of this hydrogen bond is slightly increased when guanine is paired with C, but only by ca. 2 kJ mol^{-1}, which is insufficient to account for the increase in the overall binding energy of

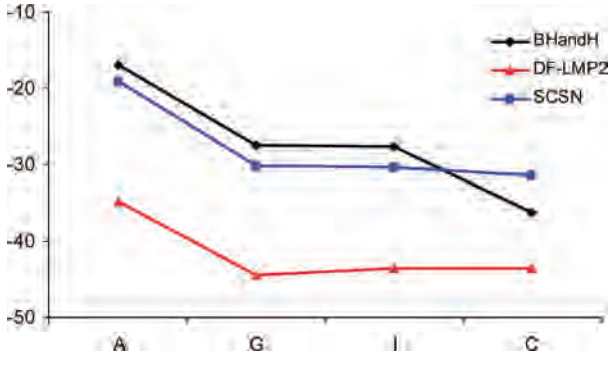

Figure 5. Binding energies of tha with nucleobases.

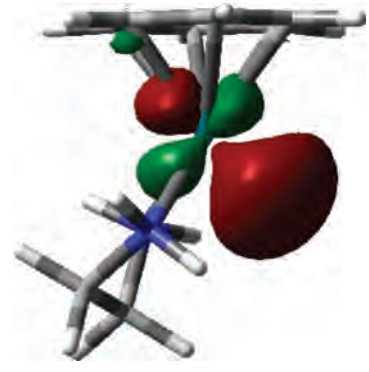

Figure 6. Representation of the LUMO of the benzene fragment, at a 0.04 au isosurface.

Table 6. Summary of AIM Analysis (au)

			arene−base	
	ρ(Ru−N_{base})	ρ(N−H···X)	$\sum\rho$(HB)[a]	$\sum\rho$(π-stack)[a]
benA	0.093	0.036		
benG	0.091	0.049		
benI	0.089	0.044		
benC	0.085	0.050		
anthA	0.091	0.032	0.010 (1)	
anthG	0.090	0.046		0.006 (1)
anthI	0.088	0.044		0.007 (1)
anthC	0.083	0.054		0.006 (1)
bipA	0.096	0.035	0.003 (1)	0.010 (1)
bipG	0.091	0.050	0.005 (1)	0.0104 (1)
bipI	0.089	0.050	0.005 (1)	0.010 (1)
bipC	0.084	0.054		0.009 (1)
dhaA	0.092	0.039	0.017 (2)	0.032 (4)
dhaG	0.091	0.046	0.008 (1)	0.031 (4)
dhaI	0.089	0.046	0.007 (1)	0.025 (3)
dhaC	0.085	0.057	0.022 (3)	0.028 (4)
thaA	0.092	0.037	0.031 (3)	0.013 (2)
thaG	0.090	0.049	0.026 (3)	0.017 (2)
thaI	0.089	0.048	0.026 (3)	0.016 (2)
thaC	0.084	0.055	0.041 (5)	0.018 (2)
benGC	0.095	0.052		
thaGC	0.093	0.054	0.040 (5)	0.033 (4)

[a] Values are the sum of the electron density at all BCPs located, with the number of BCPs in parentheses.

ruthenium found in these complexes. These hydrogen bonds are 5–10 kJ mol^{-1} stronger than the N−H···N6 bonds to adenine, which are observed in crystal structures of adenine.[92] In the pyrimidine complexes, N−H···O2 of C are of strength comparable to those seen for G and I. In this case, the second $-NH_2$ of the en ligand is also involved in rather weak (~8 kJ mol^{-1}) hydrogen bonds to C. An unexpected type of BCP was found in all C complexes, in which the N−H of the $-NH_2$ group is the donor and the Ru atom is the acceptor, as shown in Figure 6. Such hydrogen bonds to metals are not without precedent, for example, in the "inverse hydration" studied by Kozelka et al.[97,98] Using the linear relationship employed for all other hydrogen bonds, the energies of these interactions are estimated to be in the range 9–10 kJ mol^{-1}, which is of magnitude similar to that observed by Kozelka et al. However, this figure should be treated with caution because this interaction seems quite different from those used to train such relationships.

Between zero and four BCPs corresponding to arene−base stacking are also found, depending on the nature of the arene and base. These data are also summarized in Table 7. The largest number of stacking BCPs are found for dha, while in tha complexes, a number of these convert into C−H···π hydrogen bonds. In contrast, anth and bip complexes show fewer such BCPs, typically just one and, in one case (anthA), none at all. These data make it clear that the interplay of hydrogen-bonding and π-stacking effects is complex and depends on the details of both the arene and base.

Table 7 summarizes a decomposition of the overall binding energy into contributions from covalent bonding, hydrogen bonding, and π stacking, based on AIM analysis and previously established relations between the electron density and energy. Covalent energies are estimated by subtracting the hydrogen-bonding and stacking contributions from the total binding energy, assuming that the remaining energy is due to covalent bonding. These data make it clear that the bulk of the energetic preference for guanine over other bases

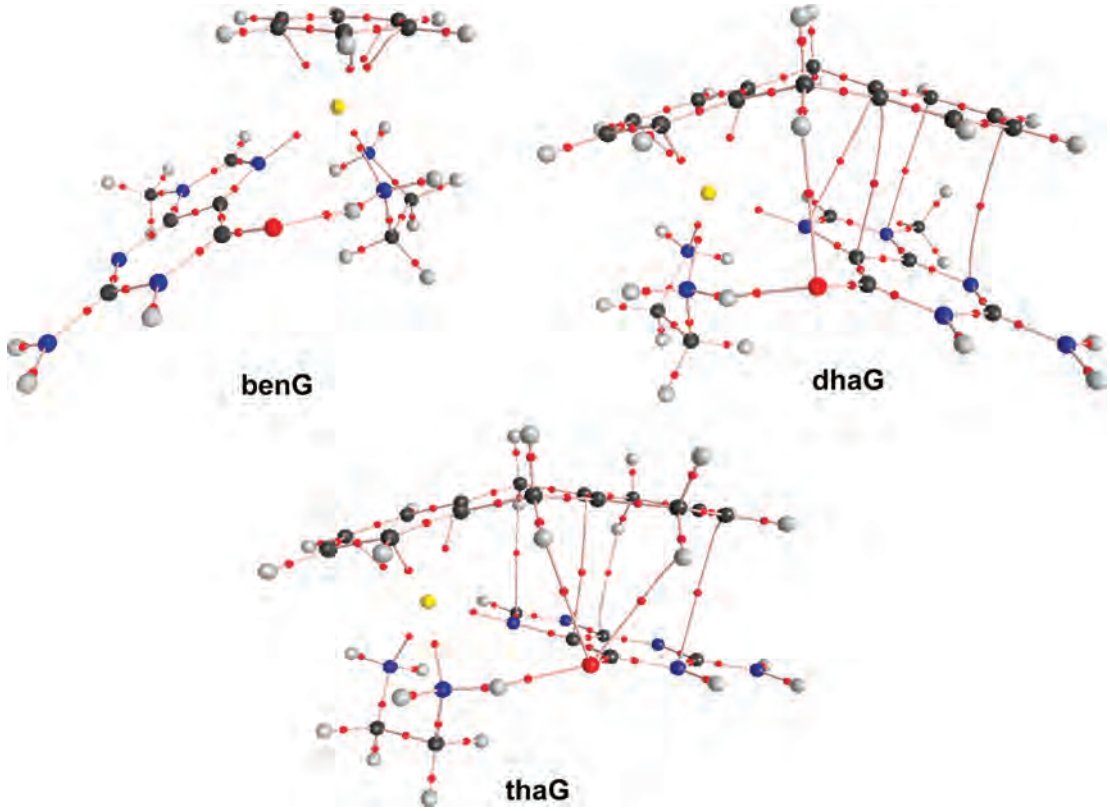

Figure 7. Molecular graphs of selected guanine complexes.

Table 7. Decomposition of the Binding Energy (BE) into Contributions from Covalent Bonding, Hydrogen Bonding, and π Stacking (kJ mol^{-1})

				arene−base	
	BE	E_{cov}	E_{enHB}	HB	stack
benA	−331.83	−309.12	−22.71	0.00	0.00
benC	−390.97	−347.72	−33.55	0.00	0.00
benG	−435.15	−404.27	−30.88	0.00	0.00
anthA	−309.71	−284.66	−20.01	−5.04	0.00
anthC	−354.66	−306.72	−33.21	0.00	−4.22
anthG	−391.82	−357.87	−29.73	0.00	−4.22
anthI	−357.06	−323.87	−28.30	0.00	−4.89
bipA	−320.05	−290.69	−22.12	0.00	−7.24
bipC	−375.49	−326.28	−33.14	0.00	−6.20
bipG	−419.75	−379.89	−32.22	0.00	−7.64
bipI	−383.03	−343.34	−32.18	0.00	−7.51
dhaA	−333.02	−277.47	−24.50	−8.12	−22.94
dhaC	−388.13	−313.25	−34.98	−9.63	−20.11
dhaG	−429.46	−373.29	−29.37	−3.75	−23.05
dhaI	−394.58	−343.78	−29.39	−3.14	−18.27
thaA	−327.15	−278.71	−23.34	−15.34	−9.76
thaC	−391.38	−315.52	−33.96	−18.42	−13.28
thaG	−430.70	−374.67	−31.54	−12.12	−12.37
thaI	−395.34	−340.68	−30.48	−12.21	−11.97
benGC	−486.03	−452.69	−33.34	0.00	0.00
thaGC	−482.53	−398.05	−35.04	−25.38	−24.06

comes from this covalent bonding. These contributions are, on average, around 34, 56, and 90 kJ mol^{-1} more favorable for guanine than for inosine, cytosine, and adenine, respectively. In contrast, noncovalent interactions are relatively constant across bases for a given arene, although the increased binding of dha and tha over anth and bip is clearly related to these noncovalent interactions.

Interestingly, we find correlations between E_{LUMO} and E_{cov} values for a given base. For all five G complexes, this yields $R^2 = 0.99$, for I complexes $R^2 = 0.98$, for C complexes $R^2 = 0.88$, and for A complexes $R^2 = 0.60$. This supports our argument that the apparently anomalous behavior of the benzene complexes is due to the electronic nature of this arene ligand, manifesting itself in lower LUMO energy on ruthenium and hence stronger binding to a given base. Some relation is also seen between E_{cov} and the electron density in the Ru−N_{base} bond, although the quality of linear correlations is rather poor because of the limited range of data available. More detail and plots can be found in the Supporting Information.

As mentioned above, binding to the GC pair is considerably more favorable that than to G alone. Table 7 shows that much of this extra stabilization comes from enhanced covalent bonding in the GC case, with a small increase in the strength of the N−H···O hydrogen bond. In the thaGC complex, further stabilization stems from stacking interactions between the arene and cytosine as well as with guanine. This is shown schematically in Figure 9. In thaG structure, the arene is positioned over guanine, whereas in thaGC, it moves slightly to be positioned over both G and C, leading to the formation of BCPs between tha and C as well as between tha and G.

(97) Bergès, J.; Caillet, J.; Langlet, J.; Kozelka, J. *Chem. Phys. Lett.* **2001**, *344*, 573–577.

(98) Barratta, W.; Mealli, C.; Herdtweck, E.; Ienco, A.; Mason, S. A.; Rigo, P. *J. Am. Chem. Soc.* **2004**, *126*, 5549–5562, and references cited therein.

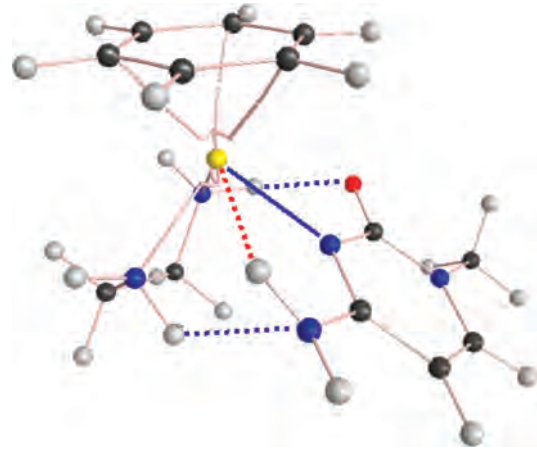

Figure 8. Molecular graph of the benC complex, with the Ru−N bond shown as a continuous blue line, hydrogen bonds shown as dashed blue lines, and the Ru···H−N interaction as a dashed red line. Other BCPs are omitted for clarity.

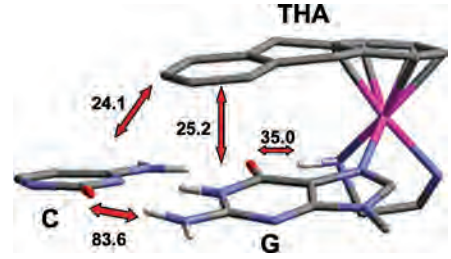

Figure 9. Noncovalent interaction energies in the thaGC complex [kJ mol^{-1}] (H atoms other than those of the G−C and G−en hydrogen bonds are not shown for simplicity).

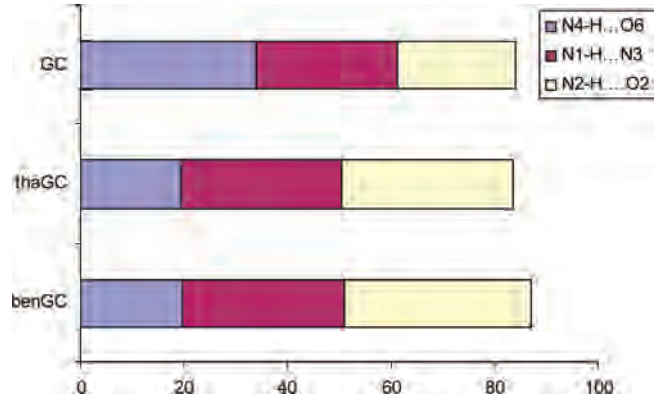

Figure 10. Individual hydrogen bond strengths in GC, benGC, and thaGC (kJ mol^{-1}).

AIM analysis can also be used to monitor the individual hydrogen bonds within the GC pairing, as shown in Figure 10. Compared to free GC, in which N4−H4···O6 is the strongest of the three hydrogen bonds present, both benGC and thaGC show substantial weakening of this hydrogen bond. In contrast, the two hydrogen bonds in which G acts as a proton donor are strengthened, such that the overall pairing energy of GC is approximately equal in all cases. This is again similar to the situation seen in complexes of cisplatin,[84] as well as other late transition metals.[99] In previous work[99] using a different set of ligands, values of 21.5, 34.7, and 36.2 kJ mol^{-1} were estimated for the

(99) Robertazzi, A.; Platts, J. A. *J. Biol. Inorg. Chem.* **2005**, *10*, 854–866.

hydrogen bonds between a Ru−G_{N7} complex and C, values only slightly different from those seen in Figure 8. From this, we suggest that ruthenium complexation to G sites in DNA should have a relatively small effect on GC pairing within the duplex.

Conclusions

We have carried out a series of DFT calculations, supported by correlated ab initio data where appropriate, to investigate the binding of ruthenium arene complexes to DNA bases. Two DFT methods reported to describe non-covalent interactions have been employed, and the results of these treatments agree on the trends in the binding energy as a function of both arene and DNA base. These data indicate a clear preference for binding at guanine over any other base, and an approximately 100 kJ mol^{-1} difference in binding between guanine and adenine, rather larger than values reported for the archetypal metal-based drug, cisplatin. However, an aqueous solution reduces this difference to around 20 kJ mol^{-1}, a value very similar to that previously reported for cisplatin. Binding to cytosine and inosine are intermediate in energy between these extremes, while comparison with thymine is complicated by the charge separation involved. DFT and ab initio data on arene−base interactions in the absence of ruthenium show that stacking and hydrogen-bonding interactions play a significant role but cannot account for all of the energy differences between bases observed.

Analysis of the calculated electron densities within the AIM framework allows further decomposition of binding energies into contributions from covalent-bonding, hydrogen-bonding, and π-stacking interactions. As expected, larger, more electron-rich arenes undergo more stabilizing stacking interactions, whereas N−H···X hydrogen bonds involving the en ligand remain rather constant. Covalent bond energies seem to be determined by the LUMO energy of the relevant Ru(en)arene fragment. AIM analysis also allows us to study the effect of ruthenium binding on GC pairing, in which individual hydrogen-bond energies are altered but the overall pairing energy remains almost constant.

Acknowledgment. Calculations were carried out at Cardiff University's Helix computational facility. This work was supported in part by EPSRC Grant ref EP/C013328/1.

Supporting Information Available: Cartesian coordinates of all optimized structures, full references for refs 54, 59, and 71, binding energies including thermal energy and entropy, and plots of E_{cov} vs E_{LUMO} and ρ(Ru−N). This material is available free of charge via the Internet at http://pubs.acs.org.

IC702459H